arXiv:hep-ph/0304296v1 30 Apr 2003

How far is normal nuclear matter from the chiral symmetry restoration? *

I.N. Mishustin,[1,2,3] L.M. Satarov,[1,2] and W. Greiner[2]

[1] *The Kurchatov Institute, Russian Research Centre, 123182 Moscow, Russia*

[2] *Institut für Theoretische Physik, J.W. Goethe Universität, D–60054 Frankfurt am Main, Germany*

[3] *The Niels Bohr Institute, DK–2100 Copenhagen Ø, Denmark*

Abstract

Properties of cold nuclear matter are studied within a generalized Nambu–Jona-Lasinio model formulated on the level of constituent nucleons. The model parameters are chosen to reproduce simultaneously the observed nucleon and pion masses in vacuum as well as saturation properties of nuclear matter. The strongest constraints on these parameters are given by the empirical values of the nucleon effective mass and compression modulus at nuclear saturation density. A preferable value of the cut–off momentum, determining density of active quasinucleon states in the Dirac sea, is estimated to about 400 MeV/c. With the most reasonable choice of model parameters we have found a first order phase transition of the liquid–gas type at subsaturation densities and the gradual restoration of chiral symmetry at about 3 times the saturation density. Fluctuations of the scalar condensate around its mean–field value are estimated and shown to be large in the vicinity of chiral transition.

PACS numbers: 11.30.Rd, 12.39.Fe, 21.65.+f

* We dedicate this work to Prof. S.T. Belyaev, the great theoretical physicist and colleague, on occasion of his 80th birthday

I. INTRODUCTION

Properties of strongly interacting matter, especially its possible phase transitions, are presently in the focus of experimental and theoretical investigations. At zero baryon density and high temperature the situation becomes more and more clear due to continuous progress in lattice calculations. Latest simulations [1] including dynamical quarks with realistic masses predict a crossover–like deconfinement (chiral) transition at temperatures around 170 MeV. The situation at finite baryon densities remains uncertain and subject to model building. Different models predict many interesting phenomena in this case, ranging from restoration of chiral symmetry to color superconductivity.

In our recent analysis [2] we tried to find phenomenological constraints on possible phase transitions at high baryon densities. The main constraint comes from the very existence of a bound state of symmetric nuclear matter at low temperature and baryon density $\rho \simeq 0.17\,\mathrm{fm}^{-3}$. We have found that predictions of some popular models are in direct contradiction with this fact. For example, several quark models predict new phases which have too low pressure as compared to ordinary nuclear matter with the same baryon chemical potential. Therefore, such phases are unstable with respect to hadronization. Our aim in this paper is to construct a QCD motivated effective model which is able to reproduce correctly the nuclear saturation point and then examine its predictions at higher densities.

Many phenomenological models have been suggested to describe properties of cold nuclear matter in terms of nucleonic degrees of freedom. The relativistic mean–field models of the Walecka type [3, 4] turned out to be rather successful in describing properties of medium and heavy nuclei. One should mention also microscopic models, dealing with nucleon–nucleon forces. Parameters of these forces are usually extracted from scattering data and the observed binding energies of light nuclei (see e.g. Ref. [5] and references therein). In addition to their numerical complexity, such approaches are essentially nonrelativistic and therefore, their accuracy diminishes at high densities. All these models have a serious drawback, namely, they do not respect the chiral symmetry of strong interactions.

There exist several chiral models which could potentially be used for describing nuclear matter. Most popular are the Nambu–Jona-Lasinio (NJL) model [6] and the linear sigma model [7]. They are able to explain spontaneous breaking of chiral symmetry in vacuum and its restoration at high energy densities. But the simplest versions of these models fail to

reproduce nuclear saturation properties. In particular, the linear sigma model predicts only abnormal state of nuclear matter [8] where the chiral symmetry is restored and nucleons have vanishing effective mass. Several more complicated models of this kind have been suggested in Refs. [9, 10, 12, 13]. Although they are able to reproduce the nuclear ground state, some new problems appear within these models. In particular, some of them do not predict restoration of chiral symmetry at high baryon densities.

There were also attempts to use the NJL model for describing cold nuclear matter [14, 15, 16] . It was argued in Refs. [14, 15] that bound nucleonic matter with spontaneously broken chiral symmetry is not possible within the standard NJL. This conclusion was based on implicit assumption that the maximum (cut–off) momentum for constituent nucleons Λ is the same as normally used in quark models ($\Lambda \sim 0.6\,\mathrm{GeV}$). The authors of Ref. [14] suggested to include additional (scalar–vector) interaction terms to reproduce the observed saturation properties of nuclear matter. On the other hand, it was shown in Ref. [16] that by assuming sufficiently low value of cutoff–momentum ($\Lambda \simeq 0.3\,\mathrm{GeV}$) it is possible to achieve a bound state at normal density even in the standard NJL model. However, in this case the nucleon effective mass at $\rho = \rho_0$ is predicted by a factor of two smaller as compared to its empirical value.

Below we reconsider the possibility of using the NJL model for describing cold nuclear matter. We use the generalized version of this model including additionally the scalar–vector interaction. We also take into account explicit symmetry breaking effects by introducing a bare nucleon mass. Indeed, with this modifications a good agreement with observed saturation properties of nuclear matter is achieved.

The paper is organized as follows. In Sect. II we formulate the model and explain the procedure of choosing parameters. Comparison of our results with observed characteristics of nuclear matter is given in Sect. III. In Sect. IV we analyze characteristics of the chiral symmetry restoration and demonstrate the importance of chiral fluctuations. In Sect. V we summarize and discuss the results.

II. FORMULATION OF THE MODEL

In this paper we return to the original formulation of the NJL model [6] in terms of nucleonic degrees of freedom. Namely, we consider a system of nucleons, interacting via

point–like scalar (pseudoscalar) and vector (axial vector) 4–fermion terms. The corresponding Lagrangian for a spinor nucleon field ψ is written as ($\hbar = c = 1$)

$$\mathcal{L}_0 = \overline{\psi}\left(i\,\partial\!\!\!/ - m_0\right)\psi + \frac{G_S}{2}\left[(\overline{\psi}\psi)^2 - (\overline{\psi}\gamma_5\boldsymbol{\tau}\psi)^2\right] - \frac{G_V}{2}\left[(\overline{\psi}\gamma_\mu\psi)^2 + (\overline{\psi}\gamma_\mu\gamma_5\psi)^2\right]\,, \qquad (1)$$

where m_0 is the "bare" nucleon mass, $\boldsymbol{\tau}$ are isospin Pauli matrices, γ^μ are standard Dirac matrices and $\gamma_5 = i\gamma^0\gamma^1\gamma^2\gamma^3$. G_S and G_V are the coupling constants for the scalar (pseudoscalar) and vector (axial vector) NN interactions, respectively.

As will be clear later, this Lagrangian is too restrictive to reproduce saturation properties of nucleonic matter at zero temperature. In particular, the model should explain the phenomenological fact that binding energy per nucleon of homogeneous isospin–symmetric matter is bound by about 16 MeV at the equilibrium density $\rho = \rho_0 \simeq 0.17\,\mathrm{fm}^{-3}$. In other words, this means that at this density the energy per baryon reaches its minimum value

$$\left.\frac{E}{B}\right|_{\rho=\rho_0} \simeq m_N - 16\ \mathrm{MeV}\,, \qquad (2)$$

where $m_N = 938\,\mathrm{MeV}$ is the nucleon mass in vacuum.

Following Refs. [9, 14], below we consider a generalized version of the NJL model including an additional 8–fermion scalar–vector (SV) interaction term. The full model Lagrangian is written as

$$\mathcal{L} = \mathcal{L}_0 + \frac{G_{SV}}{2}\left[(\overline{\psi}\psi)^2 - (\overline{\psi}\gamma_5\boldsymbol{\tau}\psi)^2\right]\left[(\overline{\psi}\gamma_\mu\psi)^2 + (\overline{\psi}\gamma_\mu\gamma_5\psi)^2\right]\,. \qquad (3)$$

It is easy to see that at $m_0 = 0$ this Lagrangian is chirally symmetric, i.e. it is invariant with respect to $SU(2)_L \otimes SU(2)_R$ transformations. Below we investigate sensitivity of nuclear matter equation of state to the coupling constants G_S, G_V and G_{SV}. In fact, they will be chosen to fulfil the condition (2).

Within the mean–field (Hartree) approximation we replace $(\overline{\psi}\Gamma\psi)^2$ operators by $2\overline{\psi}\Gamma\psi < \overline{\psi}\Gamma\psi > - < \overline{\psi}\Gamma\psi >^2$, where Γ is any combination of matrices appearing in the interaction terms of the Lagrangian (3). The angular brackets denote quantum–statistical averaging at fixed temperature T and baryon density ρ. In the considered case of isospin–symmetric matter at $T = 0$ all terms containing γ_5 vanish and the Lagrangian takes the form

$$\mathcal{L}_{\rm MFA} = \overline{\psi}\,(i\,\partial\!\!\!/ - m - \gamma^0\Sigma_V)\,\psi - U(\rho,\rho_S)\,, \tag{4}$$

where m, Σ_V and U are functions of scalar ($\rho_S =< \overline{\psi}\psi >$) and vector ($\rho =< \overline{\psi}\gamma^0\psi >$) nucleon densities. These quantities are defined as follows

$$m = m_0 - \widetilde{G}_S\rho_S\,, \tag{5}$$

$$\Sigma_V = (G_V - G_{SV}\rho_S^2)\,\rho\,, \tag{6}$$

$$U(\rho,\rho_S) = \frac{1}{2}\,(G_S\rho_S^2 - G_V\rho^2 + 3G_{SV}\rho^2\rho_S^2)\,. \tag{7}$$

In Eq. (5) we have introduced a renormalized scalar coupling

$$\widetilde{G}_S = G_S + G_{SV}\rho^2 \equiv G_S\left[1 + \alpha\,(\rho/\rho_0)^2\right]\,, \tag{8}$$

where α is a dimensionless constant, $\alpha = G_{SV}\rho_0^2/G_S$. Solutions of the gap equation (5), denoted below as m_N^*, have the meaning of the nucleon effective mass.

The Euler–Lagrange equation for the fermion field ψ has the form of Dirac equation with constant effective mass m and vector potential Σ_V. By using the plane wave decomposition of ψ one gets the explicit relations

$$\rho_S = \nu_N\int\frac{d^3p}{(2\pi)^3}\frac{m}{\sqrt{p^2+m^2}}\left[n_N(p) + n_{\overline{N}}(p) - 1\right]\,, \tag{9}$$

$$\rho = \nu_N\int\frac{d^3p}{(2\pi)^3}\left[n_N(p) - n_{\overline{N}}(p)\right]\,, \tag{10}$$

where $\nu_N = 4$ is the spin–isospin degeneracy factor for nucleons, $n_N(p)$ and $n_{\overline{N}}(p)$ are the Fermi–Dirac occupation numbers for nucleons and antinucleons. The last term (-1) in square brackets of Eq. (9) originates from the negative energy levels of the Dirac sea. It gives divergent contribution which needs to be regularized. Following common practice we do this by introducing 3–dimensional cut–off momentum Λ, i.e. replacing -1 by $-\Theta(\Lambda - p)$ where $\Theta(x) \equiv (1 + \mathrm{sgn}\,x)/2$. One can interpret Λ as maximum momentum determining the number of active quasinucleon levels in the Dirac sea [28].

From Lagrangian (4) one can easily derive the energy–momentum tensor. The energy density of homogeneous nuclear matter is written as

$$\epsilon = \nu_N\int\frac{d^3p}{(2\pi)^3}\sqrt{p^2+m^2}\,\left[n_N(p) + n_{\overline{N}}(p) - \Theta(\Lambda - p)\right] + \Sigma_V\rho + U(\rho,\rho_S) + \epsilon_0\,, \tag{11}$$

where again the three–dimensional regularization is applied to the divergent momentum integral. The constant ϵ_0 is introduced to set the energy density of the vacuum state ($\rho = 0$, $m = m_N$) equal to zero. Obviously, energy per baryon is $E/B \equiv \epsilon/\rho$.

Below we consider isospin–symmetric matter at zero temperature. In this case $n_{\overline{N}}(p) = 0$ and $n_N(p) = \Theta(p_F - p)$ where p_F is the Fermi momentum related to the baryon density,

$$\rho = \frac{\nu_N p_F^3}{6\pi^2}\,. \tag{12}$$

The scalar density reads

$$\rho_S = -\nu_N \int\limits_{p_F}^{\Lambda} \frac{d^3p}{(2\pi)^3} \frac{m}{\sqrt{p^2+m^2}} = \frac{\nu_N m}{4\pi^2}\left[p_F^2 \Phi\left(\frac{m}{p_F}\right) - \Lambda^2 \Phi\left(\frac{m}{\Lambda}\right)\right]\,, \tag{13}$$

where

$$\Phi(x) = \sqrt{1+x^2} - \frac{x^2}{2}\ln\frac{\sqrt{1+x^2}+1}{\sqrt{1+x^2}-1}\,. \tag{14}$$

At sufficiently low baryon densities corresponding to $p_F < \Lambda$ the integral in the r.h.s of Eq. (13) is positive and $\rho_S < 0$. However, at high densities, when $p_F > \Lambda$, the integral becomes negative and, therefore, $\rho_S > 0$. Then, according to Eq. (5) the nucleon effective mass becomes smaller than m_0. Of course, at large enough momenta the approximation of a point–like NN interaction will fail due to the nontrivial internal structure of nucleons. In this situation one should explicitly consider quark degrees of freedom.

Expressing ρ_S in terms of m from Eq. (5), we rewrite Eq. (11) as

$$\epsilon = -\nu_N \int\limits_{p_F}^{\Lambda} \frac{d^3p}{(2\pi)^3}\sqrt{p^2+m^2} + \frac{(m-m_0)^2}{2\widetilde{G}_S} + \frac{G_V\rho^2}{2} + \epsilon_0\,. \tag{15}$$

One can consider this expression as a functional of two independent variables, m and ρ. Then the gap equation follows from the minimization of $\epsilon(m,\rho)$ with respect to m. As has been already noticed in Ref. [14], the inclusion of SV interaction is equivalent to renormalizing the scalar coupling, $G_S \to \widetilde{G}_S$.

From thermodynamic identities at $T = 0$,

$$\mu = \frac{d\epsilon}{d\rho}\,, \quad P = \mu\rho - \epsilon = \rho^2 \frac{d}{d\rho}\left(\frac{\epsilon}{\rho}\right)\,, \tag{16}$$

one can calculate the baryon chemical potential μ and pressure P as functions of baryon density ρ. It is obvious that pressure should vanish at the saturation point, i.e. $P(\rho_0) = 0$. This gives a nontrivial constraint on the model parameters.

Our model contains five adjustable parameters, Λ, m_0, G_S, G_V, α, which we fix by fitting the vacuum masses of nucleons and pions, as well as the saturation properties of nuclear matter. First constraint follows from the gap equation in the vacuum. Taking $\rho = 0$, $p_F = 0$, $m = m_N$ in Eqs. (5), (8), (13) one has

$$m_N = m_0 - G_S \rho_S^{\rm vac} = m_0 + \nu_N G_S \frac{m_N \Lambda^2}{4\pi^2} \Phi\left(\frac{m_N}{\Lambda}\right) . \tag{17}$$

Another constraint [16] comes from the soft pion phenomenology. By using the Lagrangian (1) in the random phase approximation one can calculate the polarization operator for pionic excitations (for details see Ref. [19]). By applying further the PCAC equation for the axial–vector current of nucleons in vacuum one gets

$$m_\pi^2 f_\pi^2 = m_0 \, |\rho_S^{\rm vac}| \, , \tag{18}$$

where $m_\pi \simeq 140$ MeV and $f_\pi \simeq 93$ MeV are the vacuum values of pion mass and pion decay constant, respectively. This equation is valid in the lowest order approximation in m_π/Λ and can be considered as analogue of the Gell-Mann–Oakes–Renner relation [20] following from the quark structure of mesons. According to Eq. (18) the pure chiral limit $m_0 = 0$, used e.g. in Ref. [14], formally corresponds to vanishing pion mass.

Choosing different cut–off momenta Λ as input we use Eqs. (17)–(18) to find m_0 and G_S. The parameters G_V and α can be fixed now by the requirement that ϵ/ρ attains the minimum value (2) at $\rho = \rho_0$. At fixed Λ we first find $m = m_N^*(\rho)$ from the gap equation (see Eqs. (5), (13)) and then calculate the energy per baryon by using Eq. (15). The calculation shows that at $\Lambda \lesssim 0.2\,\mathrm{GeV}$ it is not possible to reproduce the saturation point with observable binding energy and density at any α. This becomes possible only at $\Lambda \gtrsim 0.3\,\mathrm{GeV}$ [29].

An illustration of the procedure used to determine parameters G_V and α is given in Fig. 1 for the case $\Lambda = 0.4\,\mathrm{GeV}$. At fixed α we choose the ratio $\xi \equiv G_V/G_S$ to obtain minimal energy per baryon given in Eq. (2). As one can see in this figure, increasing α shifts the minimum in ϵ/ρ to smaller baryon densities. In the considered case the choice $\alpha = 0$ leads to abnormal ($m_N^* \simeq 0$) bound state at density $\rho \simeq 2.2\rho_0$. The correct position of the saturation point is obtained for $\alpha = 0.032$. We repeat this analysis for other values of Λ from the interval $0.3\,\mathrm{GeV} < \Lambda < 0.7\,\mathrm{GeV}$.

The corresponding parameters are listed in Table I. The second and third columns give G_S and m_0 values. determined, respectively, from Eqs. (17) and (18).

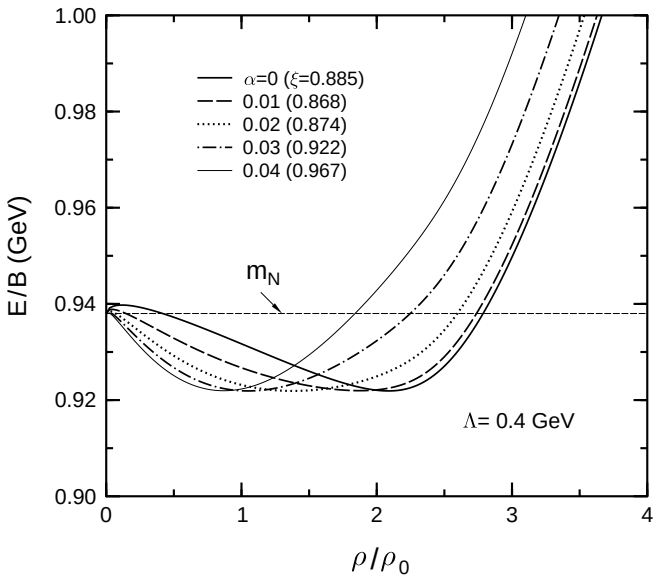

FIG. 1: Energy per baryon in cold nuclear matter as a function of baryon density ρ, calculated with the cut-off momentum $\Lambda = 0.4\,\mathrm{GeV}$. Different curves corresponds to different values of scalar–vector coupling α. The parameter ξ denotes the ratio of vector and scalar coupling constants.

TABLE I: Parameters of the NJL model

$\Lambda\,(\mathrm{GeV})$	$G_S\,(\mathrm{GeV\,fm}^3)$	$m_0\,(\mathrm{MeV})$	α	ξ
0.3	3.653	95.7	0	0.885
0.4	1.677	41.3	0.032	0.931
0.5	0.900	21.7	0.026	1.226
0.6	0.542	12.9	0.024	2.224
0.7	0.354	8.41	0.0225	4.506

The last two columns show the parameters α and ξ which give the best fit of the saturation point at fixed cut–off momentum Λ. One can see from the table that the parameter α slowly decreases with Λ at $\Lambda \gtrsim 0.4\,\mathrm{GeV}$. On the other hand, the relative strength of vector interaction ξ grows noticeably with increasing Λ. It is natural to assume that the bare nucleon mass should not be smaller than $3m_{0q}$, where $m_{0q} = (5 \pm 1)\,\mathrm{MeV}$ [21] is the isospin–averaged current mass of light quarks. From this point of view the parameter sets with $\Lambda > 0.6$ GeV should be excluded. Due to the same reason the parameter set with $m_0 = 0$

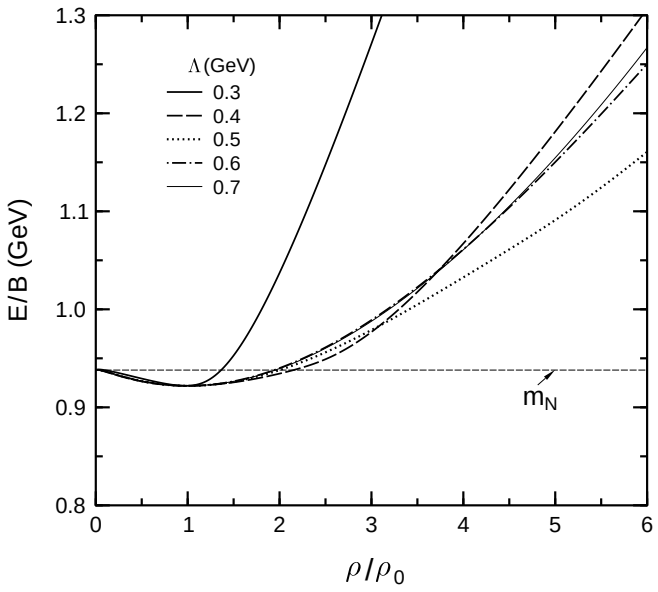

FIG. 2: Energy per baryon as a function of ρ for different Λ.

and

$$\Lambda = 0.641 \text{ GeV}\,, \quad G_S = 0.459 \text{ GeV}\,\text{fm}^{-3}\,, \quad \alpha = 0.023\,, \quad \xi = 2.92\,, \tag{19}$$

suggested in Ref. [14], does not seem reasonable.

III. NUCLEAR MATTER WITHIN THE NJL MODEL

Now we present the predictions of the generalized NJL model formulated in the preceding section. Figure 2 shows density dependence of energy per baryon calculated with parameter sets from Table I. Although the results are similar at $\rho \lesssim \rho_0$, at higher densities one can see strong sensitivity to Λ. The curve for $\Lambda = 0.3\,\text{GeV}$ shows especially large deviation from the others. As already noted above, one should be very cautious by applying the NJL model at high densities, corresponding to $p_F > \Lambda$. This is particularly important for sets with smaller Λ. Indeed, for $\Lambda = 0.3\,\text{GeV}$ $p_F > \Lambda$ holds already at $\rho > 1.4\rho_0$ [30].

Figure 3 shows density dependence of the nucleon effective mass m_N^* calculated with the same parameter sets. On can see that the m_N^* behaviour depends strongly on Λ even at low densities. For example, at $\Lambda = 0.7\,\text{GeV}$ it has a very peculiar behavior. In this case m_N^* first increases, reaching maximum value $m_N^* \simeq 1.4\,\text{GeV}$ at $\rho \simeq 10\,\rho_0$, and then drops down approaching the bare mass at $\rho \sim 17\rho_0$. For all Λ the nucleon effective mass becomes small

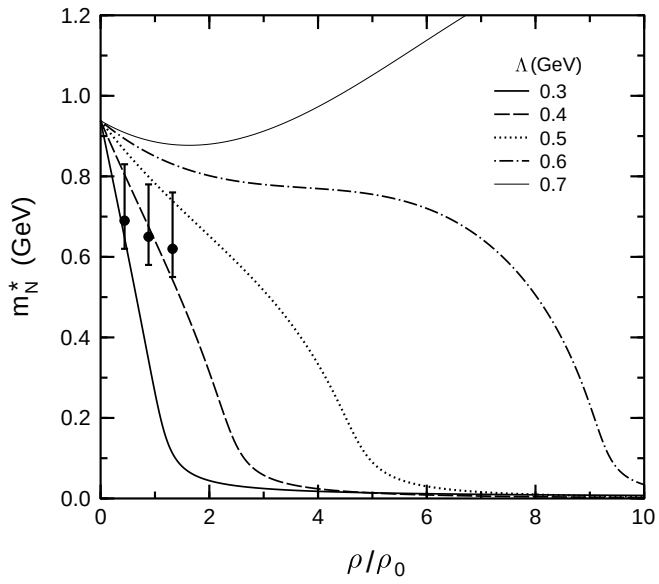

FIG. 3: Nucleon effective mass as a function of baryon density for different Λ. The dots show estimates [22], based on the QCD sum rules.

at sufficiently high densities, but it does not vanish. This would be possible only in the case of exact chiral symmetry ($m_0 = 0$) when $m_N^* = 0$ is an exact solution of the gap equation. Therefore, for all parameter sets with $m_0 \neq 0$ the chiral symmetry is only approximately restored at high densities. By filled dots in Fig. 3 we show the mass values obtained from the QCD sum rules [22]. Although the error bars are large, these estimates clearly favour the parameter set with $\Lambda = 0.4\,\mathrm{GeV}$. As compared to vacuum, a 30% reduction of the nucleon mass at $\rho = \rho_0$ is predicted in this case. The results for different Λ are presented in Table II.

TABLE II: Properties of nuclear matter within the NJL model

$\Lambda\,(\mathrm{GeV})$	$m_N^*(\rho_0)/m_N$	$K(\rho_0)\,(\mathrm{MeV})$	$\Sigma_{\pi N}\,(\mathrm{MeV})$	ρ_c/ρ_0
0.3	0.385	1350	101	1.24
0.4	0.683	285	42.1	2.66
0.5	0.834	322	25.1	5.08
0.6	0.905	347	15.9	9.51
0.7	0.944	337	10.9	16.3

The compression modulus of nuclear matter, K, is an important characteristics of the

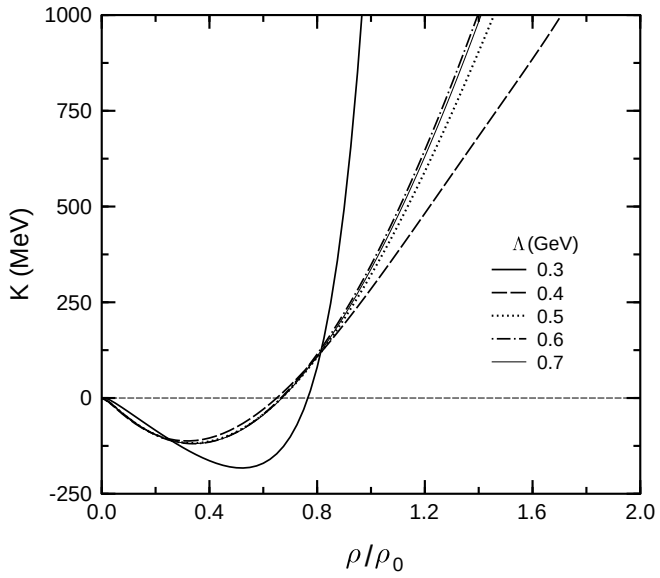

FIG. 4: Compression modulus as a function of baryon density at different Λ.

equation of state. It is defined as

$$\frac{K}{9} = \frac{dP}{d\rho} = \rho\frac{d\mu}{d\rho} = \rho\frac{d^2\epsilon}{d\rho^2}\,, \tag{20}$$

where the second and third equalities follow from Eq. (16). The density dependence of K is shown in Fig. 4 for different values of Λ. Negative K values correspond to mechanical instability of matter with respect to density fluctuations. The density interval with $K < 0$ is known as the spinodal region of a first order (liquid–gas) phase transition. As one can see from Fig. 4, this phase transition is undoubtedly predicted in all cases considered. This is not surprising because such a phase transition is a consequence of the saturating property of the equation of state. Indeed, since pressure is zero at $\rho = 0$ and $\rho = \rho_0$ is must be a nonmonotonous function of ρ. Fig. 4 also shows that the compression modulus changes very rapidly in the vicinity of the saturation point, especially in the case of $\Lambda = 0.3\,\mathrm{GeV}$. The values of K at $\rho = \rho_0$ are given in Table II. One can see that the parameter set with $\Lambda = 0.4\,\mathrm{GeV}$ gives the K value which is close to the phenomenological estimate, $K \simeq 250 - 270\,\mathrm{MeV}$ [23].

In studies of in–medium effects, the so–called pion–nucleon sigma term, $\Sigma_{\pi N}$, is often used [19, 24]. At small densities it can be defined as

$$\Sigma_{\pi N} = \left(1 - \frac{<\overline{q}q>}{<\overline{q}q>_{\mathrm{vac}}}\right)\frac{m_\pi^2 f_\pi^2}{\rho}\,, \tag{21}$$

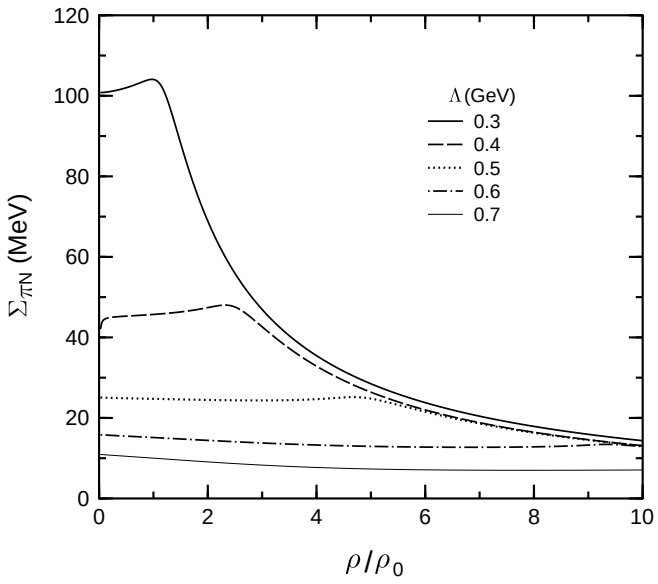

FIG. 5: Pion–nucleon sigma term as a function of baryon density at different Λ.

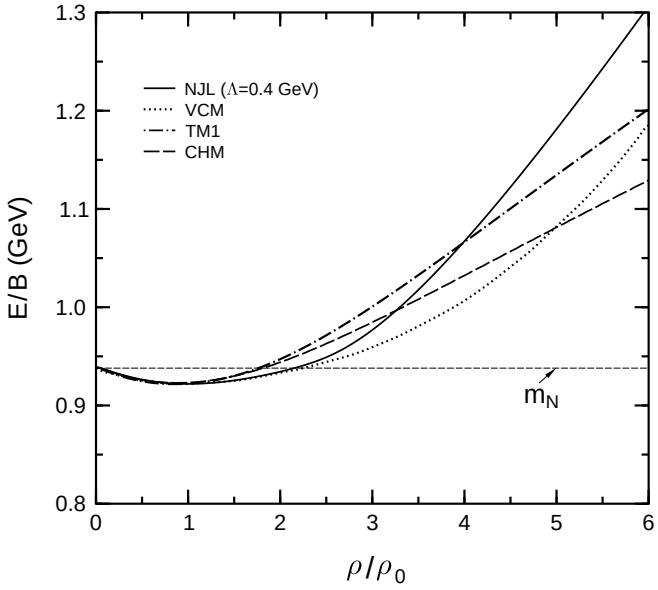

FIG. 6: Energy per baryon calculated within different nuclear models (see text).

where $< \overline{q}q >$ is the quark condensate or, in the context of our model the quark scalar density. Assuming that the scalar nucleon and quark densities are proportional to each other, we calculate $\Sigma_{\pi N}$ by using Eq. (21) with the replacement $< \overline{q}q > / < \overline{q}q >_{\rm vac} \to \rho_S/\rho_S^{\rm vac}$. The results of this calculation are shown in Fig. 5. The $\Sigma_{\pi N}$ values at $\rho \to 0$ are also given in Table II. At $\Lambda = 0.4\,{\rm GeV}$ the calculated value is close to the estimate $\Sigma_{\pi N} \simeq (35 \pm 5)\,{\rm MeV}$, obtained from the chiral perturbation theory [25].

Based on the results presented above we come to the conclusion that the generalized NJL model with $\Lambda \simeq 0.4\,\mathrm{GeV}$ gives the best description of cold nuclear matter in comparison with other choices of Λ. In Fig. 6 we compare energies per baryon predicted by our model with the results of other nuclear models namely, the Walecka–type TM1 model [26], the Chiral Hadron Model (CHM) [13] and the Variational Chain Model (VCM) [5]. Note that the VCM includes two– and three–body NN forces and takes into account the correlation effects. One can see that at densities $\rho \lesssim 2\,\rho_0$ our model and other models give very similar results. Thus, with $\Lambda = 0.4\,\mathrm{GeV}$ our fit of nuclear saturation properties is at least of the same quality as in other models listed above.

IV. IDENTIFICATION OF THE CHIRAL TRANSITION

In this section we examine properties and possible signatures of the chiral transition in cold nuclear matter. As noted in Ref. [27] the direct signature of the chiral symmetry restoration is not the effective mass (the latter may even increase with energy density), but the vanishing chiral condensate. In our approach the chiral condensate coincides with the scalar nucleon density $\rho_S = <\overline{\psi}\psi>$. Figure 7 displays this quantity calculated for the same parameter sets as before. Unlike the effective mass, $|\rho_S|$ decreases practically linearly with ρ at not too high densities. We define the critical baryon density of the chiral transition, ρ_c, by the linear extrapolation of $\rho_S(\rho)$ to zero. Numerical values of these densities (in units of ρ_0) are given in the last column of Table II.

The results of Fig. 7 suggest that scalar density curves for different Λ have similar behavior and roughly can be obtained from one another by rescaling the axes. In Fig. 8 we show the same results, but scalar and vector nucleon densities are now scaled by the factor Λ^{-3}. One can see that in these variables the results for different Λ are indeed very close to each other. It is evident now that the critical density for the chiral transition may be roughly estimated as

$$\rho_c \simeq 0.06\,\Lambda^3\,. \tag{22}$$

The corresponding Fermi momentum p_F at $\rho \simeq \rho_c$ equals approximately $0.96\,\Lambda$. Therefore, the region of the chiral transition is close to the boundary of the model applicability (see discussion above).

It is instructive to compare the vacuum value of nucleon scalar density with the quark

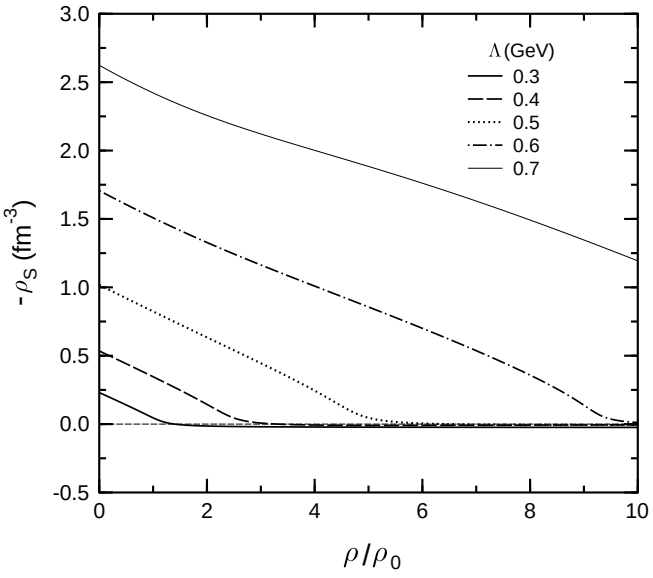

FIG. 7: Scalar condensate density as a function of baryon density for different Λ.

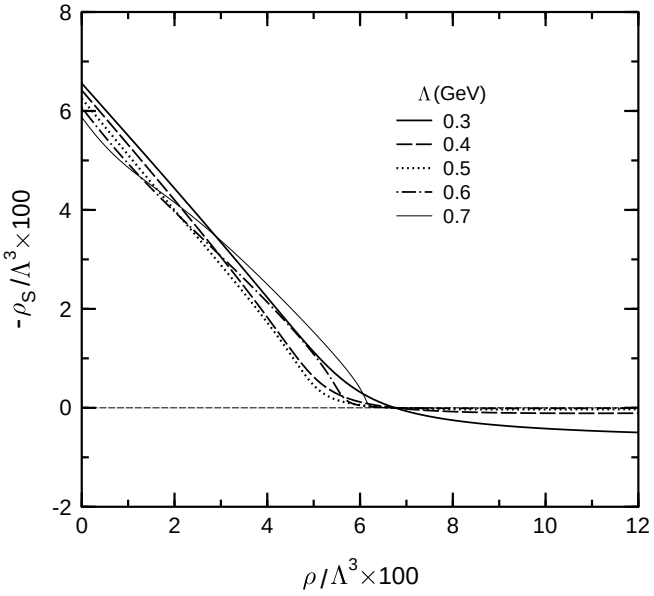

FIG. 8: Same as Fig. 7, but with scaled densities.

condensate $< \overline{q}q >$. The phenomenological value of the quark condensate in vacuum is [24]

$$| < \overline{q}q > |_{\rm vac} \simeq 2 \, | < \overline{u}u > |_{\rm vac} \simeq 2 \, (225 \pm 25 \, {\rm MeV})^3 \simeq (3 \pm 1) \, {\rm fm}^{-3} \, . \tag{23}$$

According to Fig. 7, for $\Lambda = 0.4 \, {\rm GeV}$ one gets the value $|\rho_S^{\rm vac}| \simeq 0.54 \, {\rm fm}^{-3}$ which is by about factor 6 smaller than $| < \overline{q}q > |_{\rm vac}$. For $\Lambda = 0.5 \, {\rm GeV}$ the ratio is close to 1/3 which might be expected from the naive constituent quark model. For higher Λ the predicted nucleon

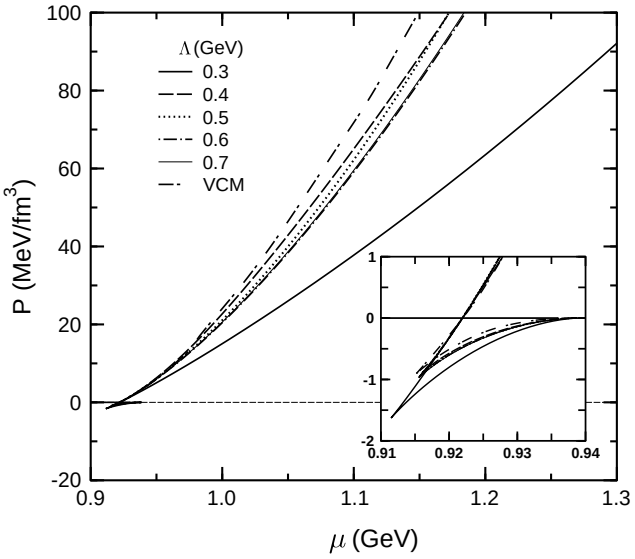

FIG. 9: Pressure as a function of chemical potential for different Λ. The curve labelled by VCM is calculated within the model of Ref. [5]. The insert shows $P(\mu)$ in the region of liquid–gas phase transition.

condensate is comparable with $< \overline{q}q >_{\rm vac}$.

When looking for possible phase transitions it is most useful to calculate pressure P as a function of chemical potential μ. A first order phase transition is signalled by appearance of several branches of $P(\mu)$. At fixed μ only the branch with highest pressure corresponds to a stable phase. The point of phase transition, $\mu = \mu_c$, is given by intersection of a stable and a metastable branches. At this point $dP/d\mu$ exhibits a jump which corresponds to difference of densities between coexisting phases. Figure 9 shows the pressure curves predicted by our model for different Λ. At small μ one can see the presence of a first–order phase transition which takes place at $\mu \simeq m_N - 16\,\mathrm{MeV} \simeq 922\,\mathrm{MeV}$ for all considered sets of model parameters. The region of mixed phase covers subnuclear densities, $\rho < \rho_0$. This is a liquid–gas phase transition which is well–known in nuclear physics. It is responsible for the multifragmentation phenomenon in hot nuclear systems. There is no clear evidence of other non–trivial behaviors of $P(\mu)$. Calculating P as a function of ρ shows that pressure varies rather smoothly at $\rho \simeq \rho_c$ i.e. in the vicinity of the chiral transition.

The results presented above were obtained assuming validity of the men–field approximation. In particular, fluctuations of the scalar condensate ρ_S or, equivalently, the nucleon effective mass m around their values determined from the gap equation were completely disregarded. As we shall see below, this approximation becomes rather poor at $\rho \sim \rho_c$. To

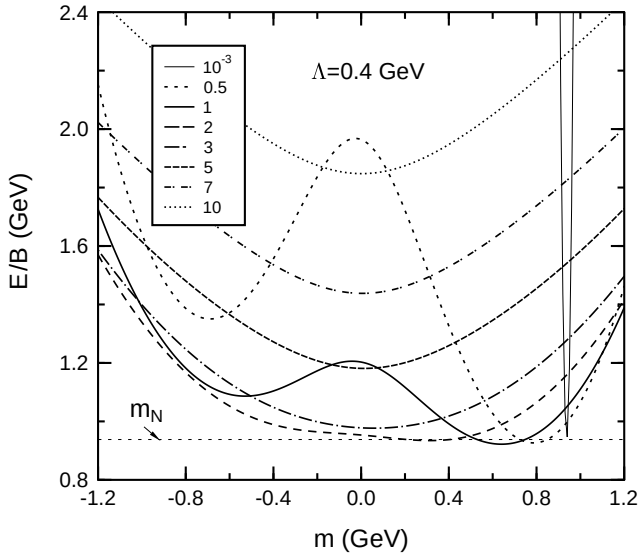

FIG. 10: Energy per baryon as a function of nucleon mass at fixed baryon densities (shown in units of ρ_0 in the key box) within the NJL model with $\Lambda = 0.4\,\mathrm{GeV}$.

estimate possible magnitude of mass fluctuations, it is instructive to study the energy per baryon, ϵ/ρ, as a functional of ρ and m, i.e. without using the gap equation. By fixing baryon density, one obtains the profiles of ϵ/ρ as functions of m. Their minima correspond to $m = m_N^*(\rho)$. The results of calculations are shown in Fig. 10 for the parameter set with $\Lambda = 0.4\,\mathrm{GeV}$.

As seen in Fig. 10, at $\rho \to 0$ energy per baryon is a sharp function of mass near its minimum at $m \simeq m_N$. As ρ grows, the minimum of ϵ/ρ shifts to smaller masses and its width significantly increases. At $\rho = \rho_0$ the minimum corresponds to the saturation point where $m = m_N^* \simeq 0.683\, m_N$. When ρ approaches the characteristic density of chiral transition $\rho \simeq \rho_c$ the minimum shifts to $m \simeq 0$ and ϵ/ρ curves become rather flat. For example, at $\rho = 2\rho_0$ the width of mass distribution becomes comparable with the value $m_N^* \simeq 0.3\,\mathrm{GeV}$ obtained from the gap equation. At higher densities widths of ϵ/ρ remain approximately the same.

To qualitatively characterize this behavior, we evaluate $\partial^2\epsilon/\partial m^2$, the second derivative of ϵ with respect to m at fixed ρ and $m = m_N^*(\rho)$. This quantity describes the stiffness of the effective potential along the mass coordinate. It is analogous to the compression modulus characterizing the stiffness with respect to the density fluctuation. The results

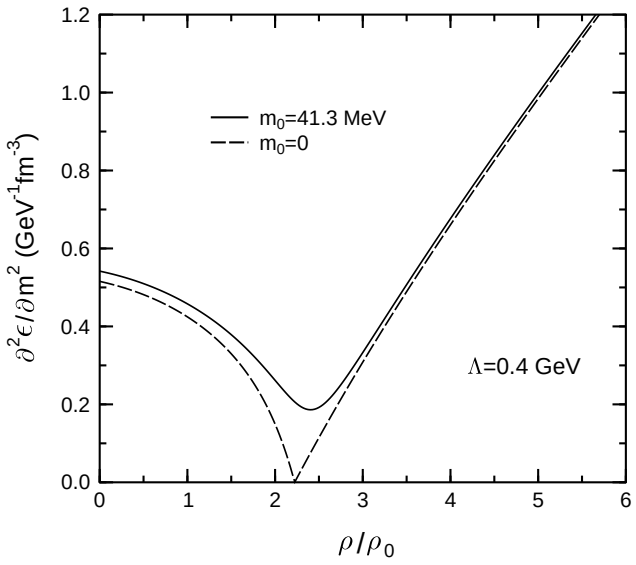

FIG. 11: Second derivative of energy density with respect to nucleon effective mass as a function of baryon density. Solid line represents the results of calculation with the parameters from second line of Table I. Dashed line corresponds to the same calculation, but with $m_0 = 0$.

are shown in Fig. 11 by the solid line. For comparison, the dashed line shows the same calculation, but with vanishing bare mass m_0. One can clearly see that the stiffness drops dramatically at the point of chiral symmetry restoration, where m_N^* and ρ_S become small. In the case $m_0 = 0$ the stiffness vanishes at $\rho = \rho_c$ and, therefore, the fluctuations diverge. Such behavior is expected for a second order phase transition. It is well known that the mean–field approximation breaks down in the vicinity of the critical point. However, in a realistic case of $m_0 \neq 0$ one can speak only about a significant enhancement of fluctuations near the chiral transition point.

Finally, in Fig. 12 we present a three–dimensional plot of ϵ/ρ as a function of m and ρ, calculated for the same set with $\Lambda = 0.4\,\mathrm{GeV}$. Thick line connecting local minima of this surface corresponds to solutions of the gap equation (5). One can easily notice approximate symmetry of ϵ/ρ with respect to reflections $m \to -m$. At low densities one sees two local minima [31] separated by a barrier (see also Fig. 10). At $\rho \simeq \rho_c$ the barrier disappears and the surface becomes rather flat along the mass axis.

It is interesting to note that in the case of exact chiral symmetry ($m_0 = 0$) the energy functional would be an even function of the effective mass m, i.e. $\epsilon(-m, \rho) = \epsilon(m, \rho)$. In particular, at $\rho \to 0$ it has two degenerate minima at $m = \pm m_N$. This symmetry is simply a particular case of the chiral rotation corresponding to angle π. By using this fact

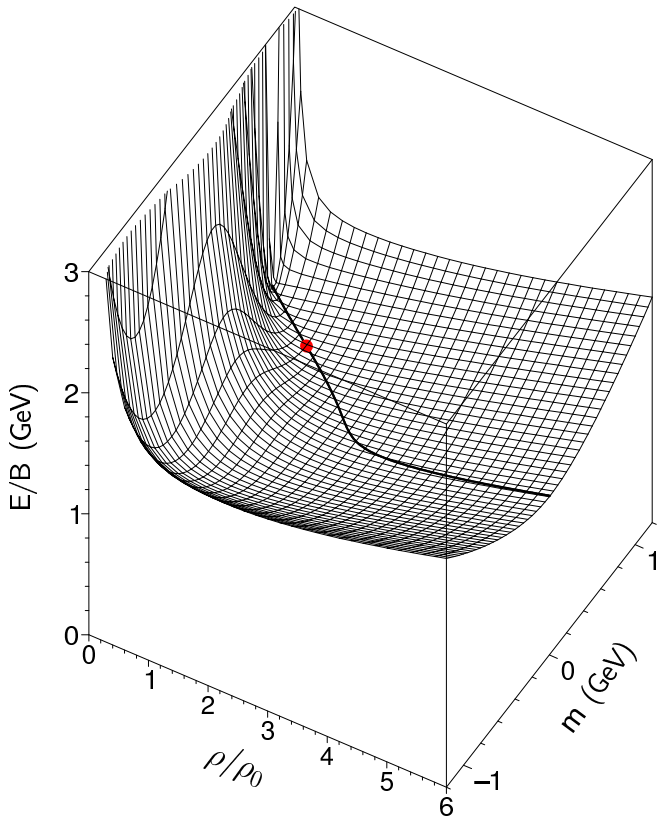

FIG. 12: Energy functional in the coordinates "effective mass–baryon density" calculated within the NJL model with $\Lambda = 0.4\,\mathrm{GeV}$. Thick line shows local minima given by the gap equation. The dot marks the global minimum corresponding to the nuclear saturation point.

one can prove the following theorem, valid also at $T \neq 0$. Namely, the thermodynamic potential of any chirally–symmetric theory, $\Omega = -P(m, T, \mu)$ is an even function of the fermion mass m and has an extremum (maximum, minimum or saddle point) at $m = 0$. Explicit symmetry breaking terms make Ω slightly tilted towards $m > 0$. All known chiral models obey this theorem. In contrast, traditional nuclear models of Walecka type strongly violate it. They assign no special significance to the point $m = 0$. Such models are tuned to the saturation point of nuclear matter and can not be extrapolated far away from this point. As an example, in Fig. 13 we show the energy surface predicted by the TM1 version of the relativistic mean–field model [26]. One can see that the model does not reveal any symmetry with respect to $m \to -m$. Moreover the minima at $m < 0$ do not appear at all.

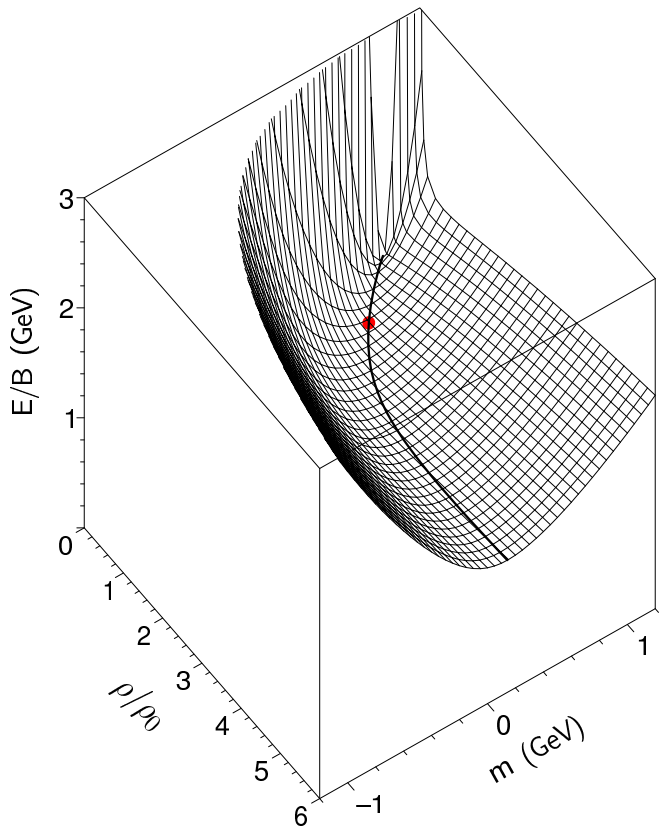

FIG. 13: Same as Fig. 12, but calculated within the TM1 model.

V. SUMMARY AND DISCUSSION

In this paper we describe cold nuclear matter using a generalized version of the NJL model including additional scalar–vector interaction terms. We formulate the model in terms of nucleonic degrees of freedom bearing in mind that normal nuclei are indeed made of nucleons. We have demonstrated that this model is able to reproduce well observed saturation properties of nuclear matter such as equilibrium density, binding energy, compression modulus and nucleon effective mass at $\rho = \rho_0$ .The best fit of nuclear properties is achieved with the cut–off momentum $\Lambda \simeq 0.4\,\mathrm{GeV}$ which is noticeably smaller than usually assumed for quark–based models. This is an indication that using nucleonic quasiparticles is only justified at low momenta $p < \Lambda$. At higher p the quark degrees of freedom should be included explicitly.

The model predicts two interesting features. First, it reveals a first order phase transition of the liquid–gas type occurring at subsaturation densities. This phase transition automatically follows from the existence of the nuclear bound state and, therefore, must be

present in any realistic model of nuclear matter. Second, the model predicts an approximate restoration of chiral symmetry at high baryon densities, $\rho \gtrsim 3\rho_0$. This feature is also quite natural for the NJL model and is expected in any chiral model. But as follows from our analysis, this chiral transition does not produce any significant peculiarities in thermodynamical quantities. Only in the case of exact chiral symmetry ($m_0 = 0$) this phenomenon would correspond to a true second order phase transition. It is demonstrated that the chiral transition is manifested by increased fluctuations of the order parameter, i.e. the scalar condensate.

We want to stress that our model is able to describe simultaneously the saturation properties of nuclear matter and restoration of chiral symmetry at high baryon densities. The model exhibits only one first order phase transition of the liquid–gas type at subsaturation densities. Restoration of chiral symmetry develops gradually with increasing baryon density and does not lead to any phase transition. This confirms conclusions of Ref. [2] where we have shown that some popular predictions of the first order chiral phase transition are incompatible with phenomenological constraints.

In conclusion, we have achieved a good description of cold nuclear matter on the basis of a relatively simple chiral model. Within this model normal nuclei are interpreted as droplets of baryon–rich matter in a phase with spontaneously broken chiral symmetry. The gradual approach to a phase with restored chiral symmetry is predicted at baryon densities above $3\rho_0$. This model can be easily extended to nonzero temperatures and finite nuclei.

Finally we want to emphasize the following. The liquid–gas phase transition discussed above can be observed via multiple production of nuclear fragments in nuclear reactions at intermediate energies. Nuclear multifragmentation is well established phenomenon and many observations reveal trends expected for such a phase transition. The situation with the chiral/deconfinement transition in baryon–rich matter is less certain. Despite of many interesting suggestions a similar unique phenomenon linked to this transition has not been established yet. We believe that effects of the chiral symmetry restoration will be most clearly seen in nuclear collisions at energies of a few 10 AGeV, when highest baryon densities are expected. But to find them one should be prepared for a thorough study of observables sensitive to chiral fluctuations.

Acknowledgments

This work has been supported by the DFG Grant 436 RUS 113/711/0-1 and the RFBR Grants 00–15–96590, 03-02-04007.

---

[1] F. Karsch, Nucl. Phys. **A698**, 199 (2002).

[2] I.N. Mishustin, L.M. Satarov, H. Stöcker, and W. Greiner, Phys. Rev. C **66**, 015201 (2002).

[3] B.D. Serot and J.D. Walecka, Adv. Nucl. Phys. **16**, 1 (1985).

[4] B.D. Serot and J.D. Walecka, Int. J. Mod. Phys. **E6**, 515 (1997).

[5] A. Akmal, V.R. Pandharipande, and D.G. Ravenhall, Phys. Rev. C **58**, 1804 (1998).

[6] Y. Nambu and G. Jona-Lasinio, Phys. Rev. **122**, 345 (1961); **124**, 246 (1961).

[7] M. Gell-Mann and M. Levy, Nuovo Cimento **16**, 705 (1960).

[8] T.D. Lee and G.C. Wick, Phys. Rev. **D9**, 2291 (1974).

[9] J. Boguta, Phys. Lett. **B120**, 34 (1983).

[10] I.N. Mishustin, J. Bondorf, and M. Rho, Nucl. Phys. **A555**, 215 (1993).

[11] G.W. Carter and P.J. Ellis, Nucl. Phys. **A628**, 325 (1998).

[12] P. Papazoglou, S. Schramm, J. Schaffner–Bielich, H. Stöcker, and W. Greiner, Phys. Rev. C **57**, 2576 (1998).

[13] P. Papazoglou, D. Zschiesche, S. Schramm, J. Schaffner–Bielich, H. Stöcker, and W. Greiner, Phys. Rev. C **59**, 411 (1999).

[14] V. Koch, T.S. Biro, J.Kunz, and U. Mosel, Phys. Lett. **B185**, 1 (1987).

[15] M. Buballa, Nucl. Phys. **A611**, 393 (1996).

[16] I.N. Mishustin, in Proc. Int. Conf. on Nuclear Physics at the Turn of Millenium (Wilderness, 1996), eds. H. Stöcker, A. Gallman, and J.H. Hamilton (World Scientific, Singapure, 1997), p. 499.

[17] S. Schmidt, D. Blaschke, and Yu.L. Kalinovsky, Phys. Rev. C **50**, 435 (1994).

[18] G. Ripka, *Quarks Bound by Chiral Fields* (Clarendon press, Oxford), 1997.

[19] U. Vogl and W. Weise, Prog. Part. Nucl. Phys. **27**, 195 (1991).

[20] M. Gell-Mann, R.J. Oakes, and B. Renner, Phys. Rev. **175**, 2195 (1968).

[21] Particle Data Group, K. Hagivara *et. al.*, Phys. Rev. D **66**, 010001 (2002).

[22] R.J. Furnstahl, X. Jin, and D.B. Leinweber, Phys. Lett. B **387**, 253 (1996).

[23] Z.Y. Ma, N. Van Giai, A. Wandelt, D. Vretenar, and P. Ring, Nucl. Phys. **A686**, 173 (2001).

[24] T.D. Cohen, R.J. Furnstahl, and D. Griegel, Phys. Rev. C **45**, 1881 (1992).

[25] J. Gasser and H. Leutwyler, Phys. Lett. B **253**, 252 (1991).

[26] Y. Sugahara and H. Toki, Nucl. Phys. **A579**, 557 (1994).

[27] H.A. Weldon, Phys. Rev. D **26**, 1394 (1982).

[28] Apparently, a more realistic treatment can be achieved by introducing a smooth form factor in the momentum space instead of a sharp cut–off at $p = \Lambda$ [17, 18].

[29] Strictly speaking at $\Lambda = 0.3\,\mathrm{GeV}$ the minimum in binding energy appears only at $\rho \leq 0.16$ fm^{-3} which is less than the ρ_0 value used in this work. However, having in mind that accuracy in ρ_0 is currently not better than 10%, we still consider such a low saturation densities as acceptable.

[30] For $\Lambda = 0.4$ and $0.5\,\mathrm{GeV}$ this takes place at $3.3\rho_0$ and $6.5\rho_0$, respectively. For $\Lambda \gtrsim 0.6\,\mathrm{GeV}$ the maximal densities become larger than $10\rho_0$. Nucleons will be completely dissolved at such high densities.

[31] More careful analysis shows that minima at negative m are in fact saddle points in 4-dimensional chiral space.